processes

MDPI

Article

Robust Fault Protection Technique for Low-Voltage Active Distribution Networks Containing High Penetration of Converter-Interfaced Renewable Energy Resources

Shijie Cui [1,2,3,4], Peng Zeng [1,2,*], Chunhe Song [1,2] and Zhongfeng Wang [1,2]

1 Key Laboratory of Networked Control System, Shenyang Institute of Automation, Chinese Academy of Sciences, Shenyang 110016, China; cuishijie@sia.cn (S.C.); songchunhe@sia.cn (C.S.); wzf@sia.cn (Z.W.)
2 State Key Laboratory of Robotics, Shenyang Institute of Automation, Chinese Academy of Sciences, Shenyang 110016, China
3 Institute for Robotics and Intelligent Manufacturing, Chinese Academy of Sciences, Shenyang 110169, China
4 University of Chinese Academy of Sciences, Beijing 100049, China
* Correspondence: zp@sia.cn; Tel.: +86-186-4203-3625

Received: 3 November 2019; Accepted: 20 December 2019; Published: 30 December 2019

Abstract: With the decentralization of the electricity market and the plea for a carbon-neutral ecosystem, more and more distributed generation (DG) has been incorporated in the power distribution grid, which is then known as active distribution network (ADN). The addition of DGs causes numerous control and protection confronts to the traditional distribution network. For instance, two-way power flow, small fault current, persistent fluctuation of generation and demand, and uncertainty of renewable energy sources (RESs). These problems are more challenging when the distribution network hosts many converter-coupled DGs. Hence, the traditional protection schemes and relaying methods are inadequate to protect ADNs against short-circuit faults and disturbances. We propose a robust communication-assisted fault protection technique for safely operating ADNs with high penetration of converter-coupled DGs. The proposed technique is realizable by employing digital relays available in the recent market and it aims to protect low-voltage (LV) ADNs. It also includes secondary protection that can be enabled when the communication facility or protection equipment fails to operate. In addition, this study provides the detail configuration of the digital relay that enables the devised protection technique. Several enhancements are derived, as alternative technique for the traditional overcurrent protection approach, to detect small fault current and high-impedance fault (HIF). A number of simulations are performed with the complete model of a real ADN, in Shenyang, China, employing the PSCAD software platform. Various cases, fault types and locations are considered for verifying the efficacy of the devised technique and the enabling digital relay. The obtained simulation findings verify the proposed protection technique is effective and reliable in protecting ADNs against various fault types that can occur at different locations.

Keywords: active distribution network; converter; digital relay; DG; fault; protection; power system; renewable energy resource

1. Introduction

Low-voltage active distribution networks (ADNs) comprising distributed generations (DG) such as photovoltaic (PV) solar system, microturbine, wind generation, mini-hydro, and fuel cell have become prominent in the energy sector especially in the existing smart grid setup. This is because

the DGs in ADNs are easy accessible, clean, and simplified structures. ADNs are a highly efficient, economic, and reliable form of power grids [1–3].

As a result of the distinct features of ADNs, the conventional power system protection approaches that assume high fault current amplitudes and one-way current flow conventions of radial networks are not adequate to operate ADNs [4].

The main challenge concerning the ADN protection appears where there are high proportion of converter-interfaced renewable energy sources (RESs). In this case, the fault current is relatively low (two times of the peak current) due to the small current rating of the semiconductor apparatuses of the power electronic converters. Consequently, the conventional overcurrent protection scheme cannot sufficiently detect these low fault currents and protect ADNs against severe damages that can be caused by potential network faults [5–8]. Although traditional overcurrent protection schemes can be utilized to protect ADNs when there is a strong main (utility) grid connection, the existing relay configurations must be cautiously attuned since the integration of DGs can challenge the harmonization of the protection plan [4,9–11].

There have been a few research works in area of fault protection for ADNs. Admittance-based ADN protection scheme is devised in [5]. Nevertheless, it could not provide an effective method for determining the precise line admittance for different fault types and places. In addition, the relay coordination was not completely presented in the work.

Network voltage-based fault protection of ADNs and microgrids (MGs) has been proposed by few studies [6,7,12,13]. The method presented in [7], for example, uses Park-transformed (d-q frame) network voltage to detect the occurrence of faults in a MG. Nevertheless, it did not measure the d-q components of the network voltages for all kinds of solid faults. It did not guarantee protection for high impedance faults (HIFs) as well. In addition, the method does not define the configuration of the relay that enables the presented protection scheme. The protection method in [13] applied the d-q components of network voltages for detecting solid faults and wavelet transform-based detection for HIFs. However, the findings of the proposed method are limited to isolated microgrids and its applicability to the ADNs was not considered.

Reference [8] proposed a protection strategy including its enabling relay to protect low voltage power networks. The strategy provides fault protection for both MGs and ADNs. Nonetheless, it might require a comparatively extensive time to sense faults in a medium voltage (MV) power grids because of the definite time grading technique it uses.

Reference [14] devised a fast communication-supported fault protection scheme and a microprocessor-based relay in MV power networks. The scheme delivers speedy and coordinated fault clearance for both ADNs and isolated MGs. Nonetheless, the strategy uses under voltage-based method of fault detection that may lead the relays to command false trip signals to circuit breakers (CBs) in case of temporary occurrence of voltage-sags, which all the time present in the power networks because of dynamic variation of load demands and volatility of RESs. Furthermore, the strategy neither guarantees protection for symmetrical HIFs nor delivers techniques for protecting buses.

This study devices a quick and robust fault protection technique for low voltage (LV) ADNs containing high penetration of converter-interfaced renewable energy resources. It uses microprocessor-based digital relay to enable the proposed protection technique. It explicitly provides the configuration of this digital relay. The digital relays operate in coordination detect and clear faults in the ADN. They exchange information with themselves and the central protection manager (CPM). The CPM also exchanges information with the ADN controllers and demand regulation systems. The devised technique provides primary and secondary protections for all solid fault types and HIFs at various possible fault points in the ADN. Numerous simulations are performed on a complete model of an actual ADN using the PSCAD software platform, for various fault locations and types, to substantiate the success of the devised protection technique and enabling relays.

The remaining sections of the study are prepared as follows. Section 2 offers the configuration of the devised fault protection relay. Section 3 presents the devised protection technique. The case studies and simulation findings are offered in Section 4. The study is summarized at the end in Section 5.

2. Configuration of the Devised Relay

In this study, a communication-aided protection technique is devised for LV active distribution networks. The devised protection technique uses a digital relay to sense the occurrence of fault and segregate the minimum section of the ADN impacted by the fault. The devised protection technique is actuated by the relay that hereafter is said to be the "ADN protection digital relay" (APDR). The focus of Section 2 is towards describing the architecture, operational units and key components of the APDR. If the APDR communicates with other APDRs, the ADN operator and additional components, it is known as a "communication-aided ADN protection digital relay" (CAPDR).

As aforementioned, the integration of DG causes ADNs or traditional distribution grids encounter a number of confronts, concerning control and protection problems. These problems can be summarized as follows:

1. bi-directional power flow
2. limited fault current magnitude
3. dynamic fluctuations of operating conditions
4. uncertainty of power generations

Thus, the traditional fault protection methods and relay algorithms are not enough and hence, the protection scheme and relay configurations must be redesigned and modified to operate ADNs safely and reliably [11]. Particularly, directional components are essential to evade unwanted tripping when faults impact a nearby protection area. The directional component of the neighboring area hastily disable its CB(s), for a specified time, to let the protection (main) components of the fault-impacted area to be activated and remove the fault. If the fault continues, on the other hand, the CB(s) of the neighboring protection area is activated to be opened as secondary protection following the primary protection reverse time-delay.

The proposed protection scheme can be realized using digital relays accessible in the market. Figure 1 illustrates the functional schematic and operational sections of the devised APDR/CAPDR that is the extended form of the relays provided in [13,14]. As depicted in Figure 1, five units present in the APDR/CAPDR: "directional unit", "solid fault detection unit", "HIF detection unit," "the trip unit," and "the auto-reclose unit."

The directional unit decides where the fault current flows using the method that will be discussed in Section 2.3. The solid fault detection unit is responsible for detecting all type of solid faults in the ADN. It uses the Park transformation of the network voltage as a fault detection signal. The detail analysis and derivation of the detection signal will be discussed in Section 2.1. The HIF detection unit is responsible for detection HIFs. It employs wavelet transform-based travelling wave fronts of the network current transients. At the end, the yields from the directional unit, solid fault detection unit, and HIF detection unit are applied to the tripping unit to decide the issuance of a tripping signal. The auto-reclosing unit is responsible for ensuring the seamless recoupling of the isolated section of the ADN to the normal section following the clearance of the fault.

2.1. Solid Fault Detection

As discussed in the previous sections, the proposed solid fault recognition methodology relies on the Park transformation of the ADN system voltage. The measured three-phase voltages at the APDR/CAPDR are first transformed to the direct(d)-axis and quadrature(q)-axis (dq) voltage components [15,16]. Any change in the three-phase voltage is observed by a change in the dq voltage

components [13]. This study uses the q-axis voltage as the detection signal and it is expressed as follows [13]:

$$V_q = \frac{2}{3} \cdot \left\{ \cos\theta \cdot V_a + \cos\left(\theta - \frac{2\pi}{3}\right) \cdot V_b + \cos\left(\theta + \frac{2\pi}{3}\right) \cdot V_c \right\} \quad (1)$$

Here, V_a, V_b, and V_c are the 3-phase voltages, and θ is the phase (transformation) angle.

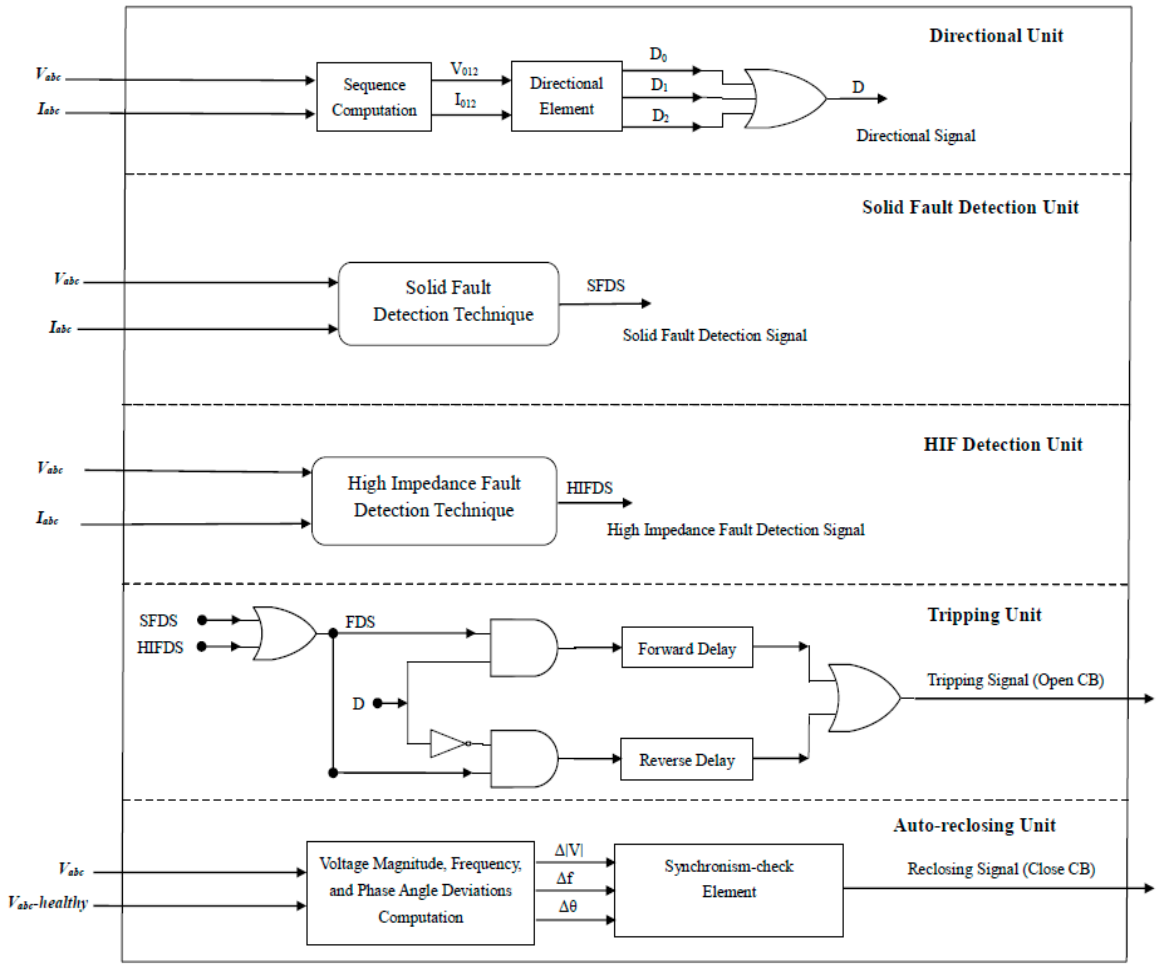

Figure 1. Schematic diagram of the communication-aided active distribution network (ADN) protection digital relay (CAPDR) and its operational units.

The disturbance voltage ($V_{q.dist}$) which is used as the fault detection signal is described as:

$$V_{q.dist} = V_{q.ref} - V_q \quad (2)$$

where, $V_{q.ref}$ is a reference q-axis voltage associated with the normal operation of the ADN before the occurrence of the fault.

Under pre-fault condition, the value of $V_{q.dist}$ is zero. When a fault occurs, $V_{q.dist}$ is a dc signal that changes based on the fault type.

For symmetrical faults, $V_{q.dist}$ is given by:

$$V_{q.dist} = V_{q.ref} - V_m \sin\varphi \quad (3)$$

where, V_m is the peak of phase voltages and φ is the phase angle.

For unsymmetrical faults, $V_{q.dist}$ is expressed as:

$$V_{q.dist} = V_{q.ref} - \{V_{Pm} \sin \varphi_P + V_{Nm} \sin(2\omega t + \varphi_N)\} \quad (4)$$

where, V_{Pm} and V_{Nm} are the maximum +ve and −ve sequence phase voltages correspondingly, ω is frequency, and φ_P and φ_N are phase angles +ve and −ve sequence phase voltage, respectively.

As observed from Equation (3), for symmetrical (three-phase) faults $V_{q.dist}$ is a DC signal. While for unsymmetrical faults, as given in Equation (4), $V_{q.dist}$ is a DC signal plus a sinusoidal component with double frequency (2ω).

Therefore, as per the devised protection technique, the solid fault detection unit of the CAPDR at the end decides the occurrence of a solid fault by contrasting the disturbance voltage ($V_{q.dist}$) with a preset threshold value. When $V_{q.dist}$ is exceeds the preset minimum level, the unit will command a solid fault detection signal (SFDS) to the trip unit of the CAPDR.

2.2. HIF Detection

The traditional overcurrent relays cannot correctly detect HIFs. Although several methodologies have been recommended by prior research works to address the problem (HIF detection) [17–19], there is no comprehensive remedy yet. This study provides a technique for HIF detection based on the observation of travelling wave fronts obtained from current transients measured at fault points (branches) [13,20].

With this technique, the 3-phase currents in the fault-impacted branches are first converted to the modal components (αβ coordinate) by employing the abc-αβ transform. Afterwards, the wave front (discrete wavelet coefficients (DWTCs)) of the modal constituents is obtained utilizing the discrete wavelet transform (DWT). The αβ branch current constituents are mainly used to obtain the propagation modes in the ADN during the fault occurrence. The DWTCs of each modal component is examined and the DWTC having the biggest amplitude is selected to decide the occurrence of the HIF. At the end, the obtained DWTC is contrasted with a preset threshold to decide they HIF occurrence. The technique has the advantage of being deployed into digital relays.

Therefore, according to the devised protection technique, the HIF detection unit of the CAPDR commands a HIF detection signal (HIFDS) to the trip unit if the fault is sensed. The fault detection signal (FDS) in the trip unit is the resultant of the logical OR of SFDS and HIFDS.

2.3. Directional Decision Forming

The devised technique uses directional units that are provided here according to the methods presented in [13,14]. When HIF happens in the ADN, the directional units cannot indicate the precise HIF point. To address this challenge, this study uses zero-sequence directional units; it is similar with the method used in [21]. In addition, negative-sequence directional unit is utilized to ensure reliable protection for unsymmetrical HIFs, for example line-to-line faults [8]. At the end, as depicted in Figure 1, directional commands from zero, −ve, and +ve sequence directional units are merged and used to generate the major directional command D. A unique delay time is employed in either direction of the relays. The relay coordination is performed by regulating the delay times.

3. Proposed Protection Technique

Here, we present the devised communication-aided protection technique, enabled by the devised relay in Section 2. The devised technique offers primary and secondary protections to solve the ADN protection challenges presented above in Sections 1 and 2.

Based on the devised protection technique, a minimal part of the ADN is separated because of the fault from the healthy section of the ADN through the commands transmitted to one or more CAPDRs. The quantity of CAPDRs used in the ADN is determined according to the preferred selectivity and

reliability needs. Every CAPDR that is responsible to protect a particular component or area dispatches 2 commands ADN protection manager (APM):

1. Fault detection signal (FDS), which indicates if the CAPDR sensed the fault inside its zone
2. Fault direction signal (D) that specifies the path of the faults from CAPDR perspective.

The calculation of the FDS and D are presented above in Sections 2.1–2.3.

The APM receives the FDS and D commands from every CAPDR and decides using a suitable logical calculation, the fault affected part of the ADN. The logical calculation is alike the "directional decision" protection technique. It is elaborated more in Section 4.

When the incidence of the fault is decided (using the FDS), the APM holds-up for a small preset period to receive another directional command and decide the fault-impacted part of the network. Afterwards, appropriate trip signal(s) are dispatched to the CB(s) linked with the CAPDR(s), to open and segregate the faulty part of the ADN. The trip commands are dispatched following a delay-time (in the range (0.1 s, 0.15 s) [22]) to provide a chance to the adjacent protection elements to operate first. This time setting can guarantee coordination of the CAPDRs with the primary protection adjacent elements.

During a CB malfunctioning, a failure command is commanded to the proximate CBs to isolate the minimum section of the ADN. The CB failure information is sent after a delay-time (in the range (0.3 s, 0.4 s) [22]) if any FDS is still active. The secondary protection is energized following a delay of 0.4 s from the fault incidence and, therefore, provides an opportunity for the aforementioned two signals to be commanded. Accordingly, if the communication malfunctions and the CAPDRs cannot get any information for a preset time, all CAPDRs will be immediately swapped to the secondary protection. The communications are not needed for the secondary protection except that it requires longer activation time than the primary protection.

The segregated (because of the fault occurrence) section of the ADN can be recoupled back and synchronized to the remaining part of the network through the resynchronization setting of its DGs and reclosing ability of its CBs if the fault is short-term and cleared immediately after the segregation.

The devised protection technique can be realized using the communication abilities of smart grids. Wireless communications [23], IEEE-802.11 wireless LAN [24] with Ethernet bridges [25] and IEC 61,850 [26] can be some of the communication channels for the application of the devised protection technique.

4. Results and Discussions

To reveal the success of the devised protection technique, the ADN whose schematic framework illustrated in Figure 2 is used. The ADN in Figure 2 is an actual LV distribution network in Shenyang, China. The network primarily delivers power to industrial park loads with a peak total demand of 5 MVA.

As depicted in Figure 2, the ADN comprises four converter-coupled DGs (CC-DGs) and two synchronous machine DGs (SM-DGs). The CC-DGs are the PV system, wind generation, vanadium redox battery (VRB) and lithium-ion (Li-Ion) battery. The capacity of each of these power sources are indicated in the figure. The SM-DGs are the diesel generator and micro gas turbine generation. Hereafter, the ADN of Figure 2 is called the "case study ADN."

All the DGs in the ADN normally operate in PQ (fixed active and reactive power) control approach as the main utility grid can always supply the reference voltage and frequency. The detail control approaches of the DGs can be referred from [27].

As presented above in Sections 2 and 3, every CAPDR sends 2 signals, FDS and D, to the APM. The APM analyses these signals received from the CAPDRs and determines the precise fault point. Then, the trip signals will be sent to the responsible CB(s) to segregate the fault-impacted part of the ADN following a preset delay-time. Table 1 provides the CAPDRs used for the primary and secondary protections to sense and remove fault from the ADN. During the occurrence faults in the ADN, the D

and FDS commands of the corresponding (adjacent) CAPDR(s) are dispatched to the APM. The fault is assumed forward fault if the FDS and D commands have a value of one.

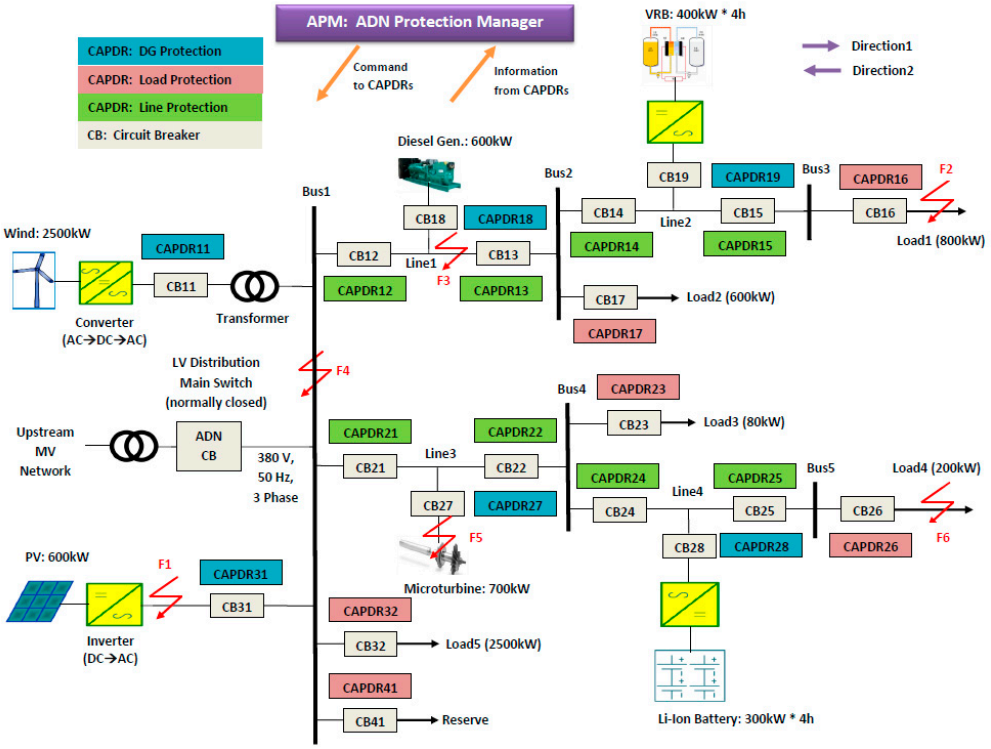

Figure 2. Model of the case study ADN with embedded CAPDRs.

Table 1. Relays and their respective protection responsibility in the case study ADN.

Fault Point		Direction 1		Direction 2	
		Primary	Secondary	Primary	Secondary
DG	Wind	CAPDR 11			
	PV	CAPDR 31			
	Diesel	CAPDR 18			
	Microturbine	CAPDR 27			
	VRB	CAPDR 19			
	Li-Ion	CAPDR 28			
Load	Load 1	CAPDR 16	CAPDR 15	N/A	
	Load 2	CAPDR 17	CAPDR 13	N/A	CAPDR 14
	Load 3	CAPDR 23	CAPDR 22	N/A	CAPDR 24
	Load 4	CAPDR 26	CAPDR 25	N/A	
	Load 5	CAPDR 32	N/A	N/A	CAPDR 12 CAPDR 21
	Reserve	CAPDR 41	N/A	N/A	CAPDR 12 CAPDR 21
Line	Line 1	CAPDR 12	N/A	CAPDR 13	CAPDR 21 CAPDR 14
	Line 2	CAPDR 14	CAPDR 13	N/A	
	Line 3	CAPDR 21	N/A	CAPDR 22	CAPDR 12 CAPDR 24
	Line 4	CAPDR 24	CAPDR 22	N/A	
Bus	Bus 1	N/A		CAPDR 12 CAPDR 21	CAPDR 13 CAPDR 22
	Bus 2	CAPDR 13	CAPDR 12	CAPDR 14	N/A
	Bus 3	CAPDR 15	CAPDR 14	N/A	
	Bus 4	CAPDR 22	CAPDR 21	CAPDR 24	N/A
	Bus 5	CAPDR 25	CAPDR 24	N/A	

To confirm the efficacy of the devised ADN protection technique and its enabling digital relay, the case study ADN, depicted in Figure 2, is modeled and simulated using the PSCAD simulation platform [28]. For CAPDRs in the major protection, the delay-times are set as 100 ms. This offers sufficient time for the tripping unit not to send false signal for temporary voltage dips in the network. The time-delay CAPDRs/APDRs in the secondary protection is set as 400 ms. The CBs need 20 ms for opening or closing. In addition, the CAPDRs are implemented with double-setting directional units in order to provide both primary and secondary protections when needed.

Likewise, the reverse time-delays of CAPDRs are set according to common practices and the techniques provided in [8] and obviously have dissimilar values from the forward time-delays since there might be distinct DG and load in the reverse direction. The q-axis reference voltage is set as the q-axis rated value. The threshold voltage is taken as 50% of the rated voltage for double line to ground (DLG), 3-line to ground (3LG) and line-to-line (LL) faults, while 20% is used for single line to ground (LG) fault. The Daubechies 8 (Db8) DWT with a sampling frequency of 6 kHz and multiresolution analysis (MRA) of unity resolution is used for the HIF detection.

The simulations consist of faults at various points in the ADN. These faults are F1, F2, F3, F4, F5, and F6 (illustrated in Figure 2) which designate faults at the PV DG terminal, Load1 terminal, distribution line, bus, microturbine DG terminal, and Load4 terminal, correspondingly. All solid faults (LG, DLG, LL, and 3LG) and HIFs are considered in the protection simulation. A resistance value of 60Ω is employed to simulate the HIFs.

For the photovoltaic DG, the primary protection is provided by CAPDR31 while F1 happens near to its terminal. Figure 3 illustrates the 3-phase voltages and q-axis disturbance voltage observed at CB31 while F1 (3LG) occurs. As observed in Figure 3, the disturbance voltage has varied considerably when F1 happened, and surpassed the preset threshold level. As shown, the disturbance voltage is a fixed DC value for a 3LG fault. As Figure 3 shows, F1 happened at 2 s and remained for 0.05 s. The CAPDR sensed F1 using the substantial variation in the q-axis voltage and dispatched the trip command at 2.02 s. CB31 opened at 2.025 s to cut off the DG and segregate it from the remaining part of the ADN. F1 cleared at 2.05 s and the CB reclosed at 2.07 s. It is shown that the ADN voltage has recovered its normal value straightaway following the disappearance of F1 through the reclose function of the devised relay. It demonstrates the rapidity of the devised technique and its quick information exchange capability.

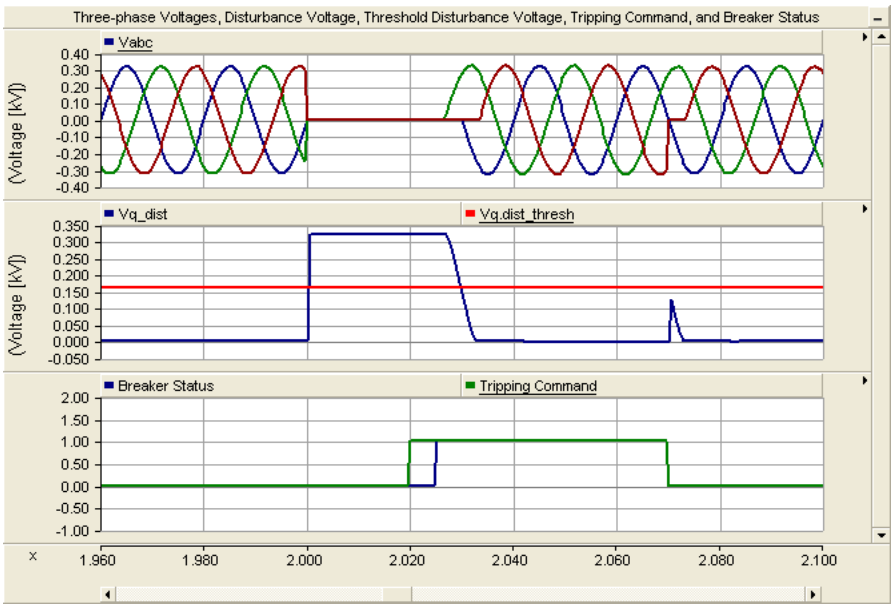

Figure 3. 3-phase voltages, disturbance voltage, and trip signal for fault 1 (F1).

For Load1, primary protection in direction1 is provided by CAPDR16 and secondary protection by CAPDR15 when F2 happens. Figure 4 depicts the 3-phase voltages, q-axis disturbance voltage, and DWTC (wave front) of current-transient observed at CB16, while F2 (DLG HIF) occurs. As shown in Figure 4, the q-axis voltage altered very little when F2 happened. It is smaller than the preset threshold level. Consequently, the q-axis disturbance voltage cannot sufficiently activate the CAPDR to dispatch a tripping command to the responsible CB. Nevertheless, the DWTC has revealed a substantial variation (surpasses the zero threshold level) while the DLG HIF (F2) happened. F2 happened at 2 s. The CAPDR has sensed F2 using the substantial alteration of the DWTC and sent trip signal to CB16 to cut off Load1 and separate it from the healthy part of the ADN.

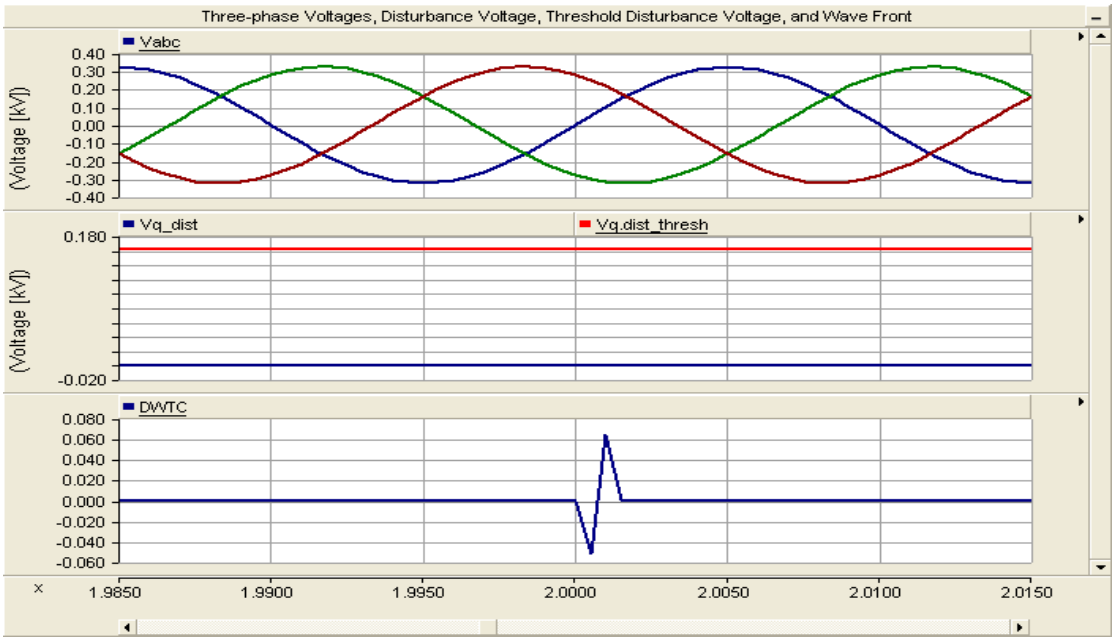

Figure 4. 3-phase voltage, disturbance voltage, and discrete wavelet coefficient (DWTC) of current transient during F2.

CAPDR12 in direction1 and CAPDR13 in direction2 are in charge of the primary protection for Line1 when F3 happens. CAPDR21 for CAPDR12 and CAPDR14 for CAPDR13 are the corresponding secondary protections in direction2. Figure 5 depicts the 3-phase voltages and q-axis disturbance voltage observed at CB13 when F3 (LG) happens. As clearly seen, the q-axis voltage varies considerably while F3 has happened and surpasses the preset threshold. The q-axis voltage in this case is a DC signal plus a ripple element with a double frequency. F3 happened at 2 s and remained for 0.05 s. Both CAPDRs sensed F3 and sent trip commands at 2.02 s. CB12 and CB13 opened at 2.025 s to separate Line1 and separate it from the healthy part of the ADN. F3 cleared at 2.05 s and the CBs reclosed at 2.07 s.

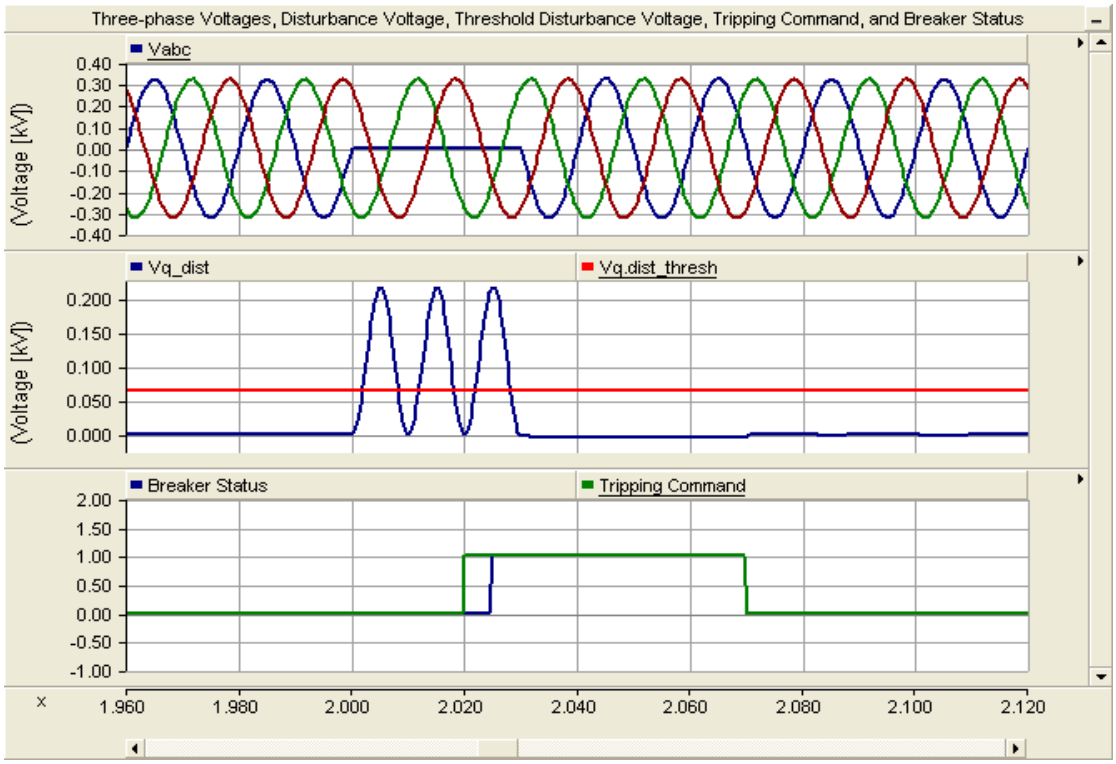

Figure 5. 3-phase voltages, disturbance voltage, and trip signal for F3.

CAPDR12, CAPDR21, CAPDR32, and CAPDR41 are in charge of primary protection of Bus1 when F4 happens. The APM determines bus faults using the direction commands (Ds) obtained from the CAPDRs coupled with the bus. It decides the incidence of the bus fault if all the Ds sent from every relay coupled with the bus are negative one (−1). The trip commands are then dispatched to all responsible CBs. Figure 6 depicts the 3-phase voltages, q-axis disturbance voltage, and current DWTC observed at CB21, while F4 (LL HIF) occurs. Similar outcome can be attained at CB12, CB32, and CB41 as well. As shown, the DWTC surpasses the zero threshold when F4 happened. F4 happened at 2 s. The CAPDRs sensed F4 and sent the trip commands to the responsible CBs to segregate Bus1 from the remaining part of the ADN.

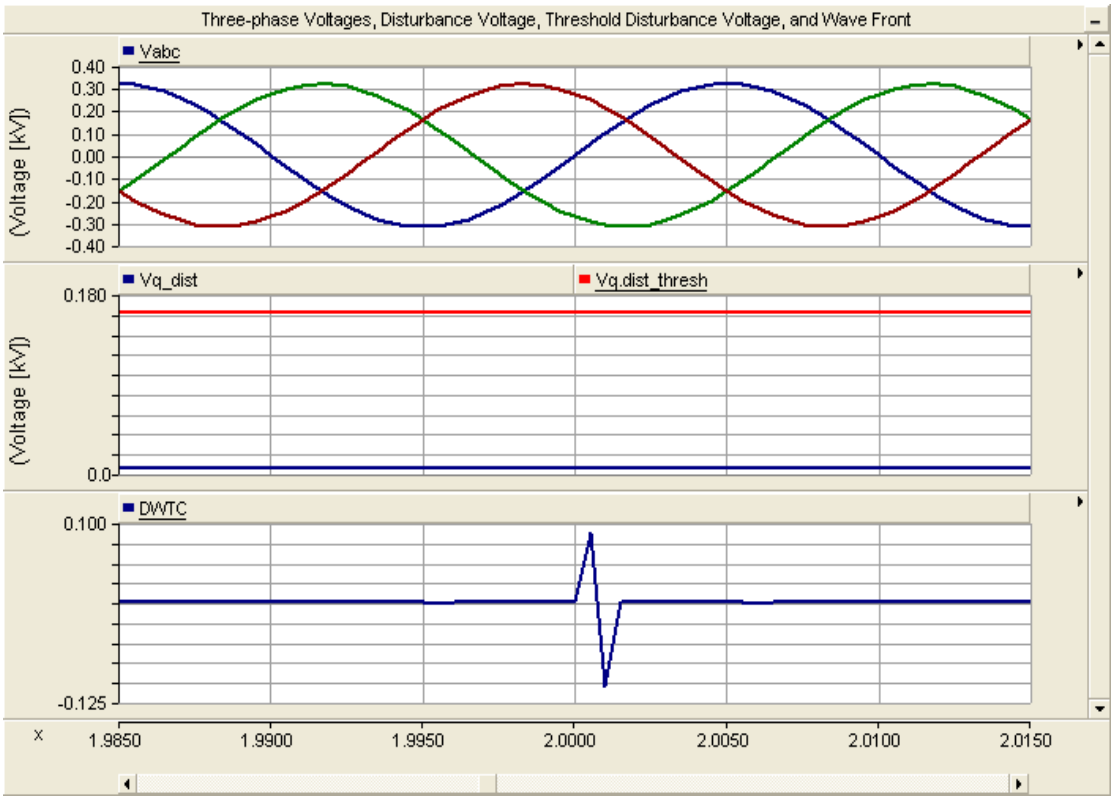

Figure 6. 3-phase voltage, disturbance voltage, and DWTC during F4.

Similarly, Figures 7 and 8 illustrate the 3-phase voltages and q-axis disturbance voltage observed at CB27 when F5 (3LG) occurs and at CB26 when F6 (LG) occurs, respectively.

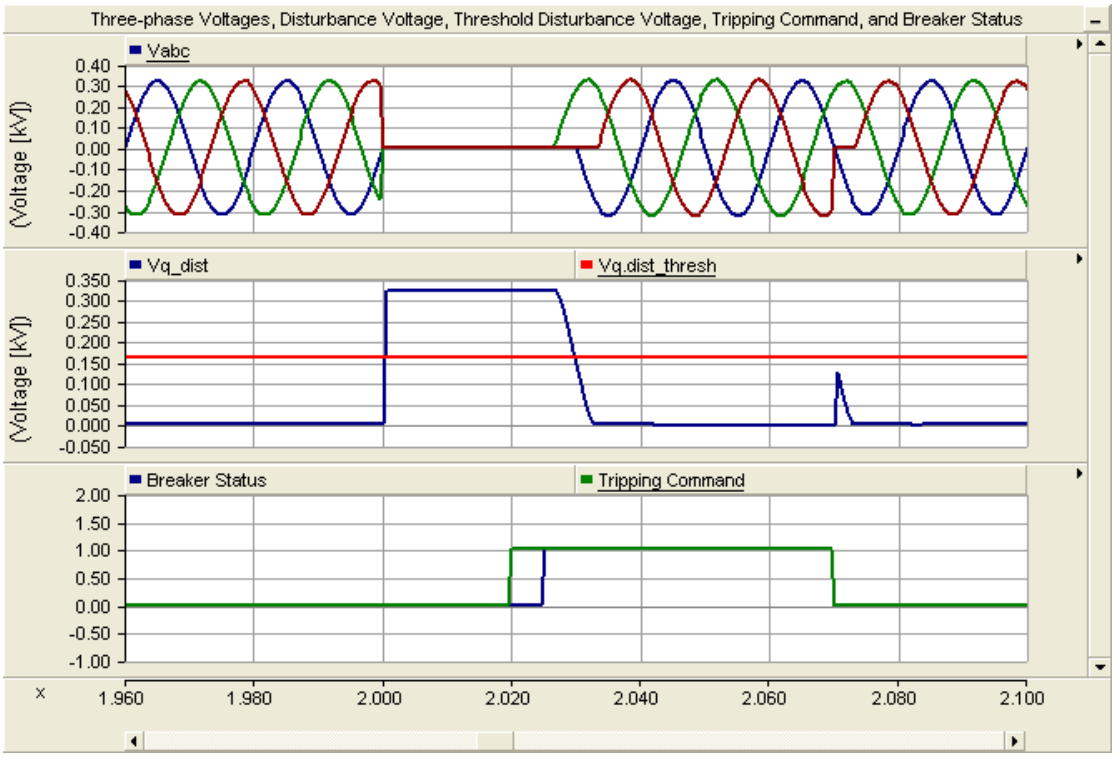

Figure 7. 3-phase voltages, disturbance voltage, and trip signal for F5.

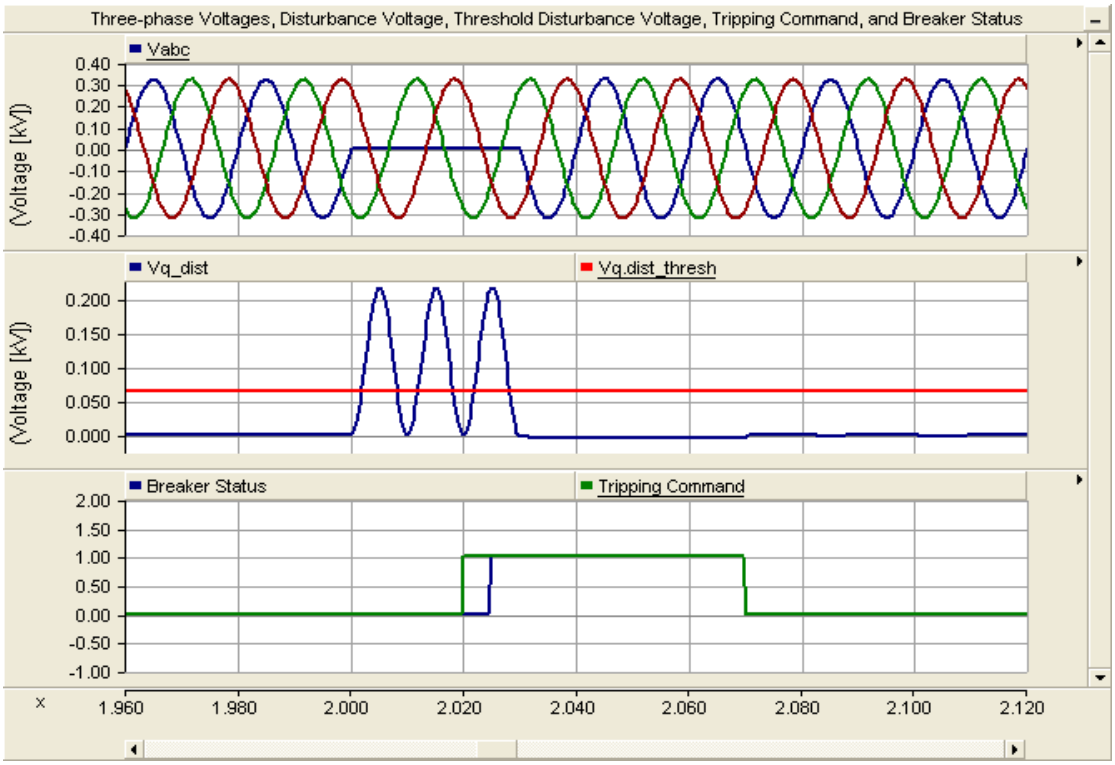

Figure 8. 3-phase voltages, disturbance voltage, and trip signal for F6.

5. Conclusions

We devised a novel communication-aided technique for quick and reliable protection of low voltage converter-dominated and renewable energy-integrated active distribution networks. The technique employs distinct approaches to detect the incidences of solid faults and HIFs. The proposed method solves the challenges brought to ADNs due to small-magnitude fault currents. It also provides both main and backup protections embedded into a proposed digital relay. The devised digital relay has five distinct units with different functions. The relay identifies diverse fault types based on the features of the disturbance voltage. The technique does not require adaptive elements. Plenty of simulations have been executed by employing the PSCAD software platform for various cases and fault locations, to reveal the efficacy of the devised fault protection technique and the actuating digital relay. The devised protection technique is successful irrespective of the position, capacity, and type of the DGs in the ADN. In addition, it is valid for any fault current amplitude, impedance, type, and point.

Author Contributions: S.C. and P.Z. modeled the ADN simulation model, formulated and implemented the protection technique; C.S. and Z.W. accomplished the management and progress evaluations of the work. All authors have checked and agreed the final version. All authors have read and agreed to the published version of the manuscript.

Funding: The research was funded by the National Key R&D Program of China (2017YFB0902900 & 2017YFB0902901), National Natural Science Foundation of China under Grant 61803368, China Postdoctoral Science Foundation under Grant 2019M661156, and Liaoning Provincial Natural Science Foundation of China under Grant 20180540114.

Acknowledgments: The work is supported by the National Key R&D Program of China (2017YFB0902900 & 2017YFB0902901), National Natural Science Foundation of China under Grant 61803368, China Postdoctoral Science Foundation under Grant 2019M661156, and Liaoning Provincial Natural Science Foundation of China under Grant 20180540114.).

Conflicts of Interest: The authors declare no conflict of interest.

Acronyms

ADN	active distribution network
APDR	ADN protection digital relay
APM	ADN protection manager
CC-DG	converter-coupled DG
DG	distributed generation
F	fault
PSCAD	power system computer-aided design
HIF	high impedance fault
dq	d-axis ~ q-axis reference frame
ESS	electrical energy storage
ADNPDR	ADN protection digital relay
CAPDR	communication-aided ADN protection digital relay
abc	three phase reference frame
αβ	alpha-beta reference frame
MG	microgrid
MRA	multi-resolution analysis
MV	medium voltage
DWT	discrete wavelet transform
V_a, V_b and V_c	phase a, b and c voltages, respectively
V_α and V_β	alpha and beta axis voltages, respectively
V_d and V_q	d-axis and q-axis voltages, respectively
$V_{q.dist}$	disturbance voltage signal
$V_{q.ref}$	q-axis reference voltage
V_m	max phase voltage
n	harmonic order
ω	angular frequency of system voltage
f	frequency
φ	initial phase angle of the system voltage
ω_r	angular frequency of the stator voltages
θ	rotor angle of rotation
DC	direct current
V_0	zero-sequence voltage
V_{Pm} and V_{Nm}	peak values of the positive- and negative-sequence fundamental voltages
φ_P and φ_N	initial phase angle values of the positive- and negative-sequence voltages
SFDS	solid fault detection signal
DWTC	discrete wavelet transform coefficient
HIF	high impedance fault
HIFDS	high impedance fault detection signal
FDS	fault detection signal
D	main directional command
D_0, D_2, D_1	zero-, negative-, and positive-sequence directional signals, respectively
DWT	discrete wavelet transform
CB	circuit breaker
CPM	central protection manager
LAN	local area network
LV	low voltage
IEEE	institute of electrical and electronic engineers
IEC	international electro-technical commission
MVA	mega volt ampere
N/A	not applicable
SM-DG	synchronous machine-based DG
VRB	vanadium redox flow battery
Li-Ion	lithium-ion battery
PQ	active-reactive power

U/f	voltage/frequency
PV	photovoltaic
ms	milli second
LG	single-line-to-ground
DLG	double-phase-to-ground
LL	line-to-line
3LG	three-phase-to-ground
Db8	Daubechies 8 wavelet
kHz	killo herz
s	second
RES	renewable energy resource
R&D	research and development
$V_{q.dist\_thresh}$	threshold disturbance voltage signal
V_{abc}	three phase voltages
I_{abc}	three phase currents
V_{012}	zero-, positive-, and negative-sequence voltages
I_{012}	zero-, positive-, and negative-sequence currents
$V_{d.ref}$	d-axis reference voltage
$V_{abc\_healthy}$	three phase voltages of non-fault-impacted or healthy section
$\Delta\|V\|$	voltage magnitude deviation
Δf	frequency deviation
$\Delta\theta$	phase angle deviation

References

1. Li, H.; Eseye, A.T.; Zhang, J.; Zheng, D. Optimal energy management for industrial microgrids with high-penetration renewables. *Prot. Control Mod. Power Syst.* **2017**, *2*, 12. [CrossRef]
2. Kishore, T.S.; Singal, S.K. Optimal economic planning of power transmission lines: A review. *Renew. Sustain. Energy Rev.* **2014**, *39*, 949–974. [CrossRef]
3. Cicconi, P.; Maneri, S.; Bergantino, N.; Raffaeli, R.; Germani, M. A design approach for overhead lines considering configurations and simulations. *Comput. Aided Des. Appl.* **2019**, *17*, 797–812. [CrossRef]
4. Butler-Purry, K.L.; Funmilayo, H.B. Overcurrent protection issues for radial distribution systems with distributed generators. In Proceedings of the IEEE PES General Meeting, Calgary, AB, Canada, 26–30 July 2009; pp. 1–5.
5. Dewadasa, M.; Ghosh, A.; Ledwitch, G.; Wishart, M. Fault isolation in distributed generation connected distribution networks. *IET J. Gen. Tran. Dist.* **2011**, *5*, 1053–1061. [CrossRef]
6. Tumilty, R.M.; Brucoli, M.; Green, T.C. Approaches to network protection for inverter dominated electrical distribution systems. In Proceedings of the 3rd IET PEMD, Dublin, Ireland, 4–6 April 2006; pp. 622–626.
7. Al-Nasseri, H.; Redfern, M.; Li, F. A voltage based protection for micro-grids containing power electronic converters. In Proceedings of the IEEE PES General Meeting, Montreal, QC, Canada, 18–22 June 2006; pp. 1–7.
8. Zamani, M.A.; Sidhu, T.S.; Yazdani, A. A protection strategy and microprocessor-based relay for low-voltage microgrids. *IEEE Trans. Power Deliv.* **2011**, *26*, 1873–1883. [CrossRef]
9. Hui, W.; Li, K.K.; Wong, K.P. An adaptive multiagent approach to protection relay coordination with distributed generators in industrial power distribution system. *IEEE Trans. Ind. Appl.* **2010**, *46*, 2118–2124.
10. Perera, N.; Rajapakse, A.D.; Buchholzer, T.E. Isolation of faults in distribution networks with distributed generators. *IEEE Trans. Power Deliv.* **2008**, *23*, 2347–2355. [CrossRef]
11. Amin, Z.; Tarlochan, S.; Amir, Y. A strategy for protection coordination in radial distribution networks with distributed generators. In Proceedings of the IEEE PES General Meeting, Providence, RI, USA, 25–29 July 2010; pp. 1–8.
12. Hou, C.; Hu, X. A study of voltage detection based fault judgment method in microgrid with inverter interfaced power source. In Proceedings of the International Conference on Electrical Engineering, Shenyang, China, 5–9 July 2009.

13. Zheng, D.; Eseye, A.; Zhang, J. A communication-supported comprehensive protection strategy for converter-interfaced islanded microgrids. *Sustainability* **2018**, *10*, 1335. [CrossRef]
14. Zamani, M.A.; Yazdani, A.; Sidhu, T.S. A Communication-Assisted Protection Strategy for Inverter-Based Medium-Voltage Microgrids. *IEEE Trans. Smart Grid* **2012**, *3*, 2088–2099. [CrossRef]
15. Edith, C. *Circuit Analysis of AC Power Systems*; Wiley: New York, NY, USA, 1950; Volume 1, p. 81.
16. Park, R.H. Two-reaction theory of synchronous machines: Generalized method of analysis, part I. *Trans. AIEE* **1929**, *48*, 716–727.
17. Christie, R.D.; Zadehgol, H.; Habib, M.M. High impedance fault detection in low voltage networks. *IEEE Trans. Power Deliv.* **1993**, *8*, 1829–1836. [CrossRef]
18. Aucoin, B.M.; Russell, B.D. Distribution high impedance fault detection utilizing high frequency current components. *IEEE Trans. Power Appar. Syst.* **1982**, *PAS-101*, 1596–1606. [CrossRef]
19. Jeerings, D.I.; Linders, J.R. Unique aspects of distribution system harmonics due to high impedance ground faults. *IEEE Trans. Power Deliv.* **1990**, *5*, 1086–1094. [CrossRef]
20. Perera, N.; Rajapakse, A.D.; Muthumuni, D. Wavelet Based Transient Directional Method for Busbar Protection. In Proceedings of the International Conference on Power Systems Transients (IPST2011), Delft, The Netherlands, 14–17 June 2011.
21. Meyer, B. *Directional Ground and Sensitive Ground Fault Settings*; Cooper Power Systems, Cooper Industries: Houston, TX, USA, 2004; pp. 1–17. Available online: https://studylib.net/doc/13718297/directional-ground-and-sensitive-ground-fault-settings--r (accessed on 1 November 2019).
22. IEEE Rec. Practice for Protection & Coordination of Industrial and Commercial Pwr. Sys., IEEE Standard. 242. 1986. Available online: https://standards.ieee.org/standard/242-2001.html (accessed on 1 November 2019).
23. Palak, P.P.; Mitalkumar, G.K.; Tarlochan, S.S. Opportunities and challenges of wireless communication technologies for smart grid applications. In Proceedings of the IEEE PES General Meeting, Providence, RI, USA, 25–29 July 2010; pp. 1–7.
24. IEEE Std. for IT, Telecoms. and Info. Exchange b/n Sys., Local and Metropolitan Area Ntks., IEEE Standard. 802.11. 2007. Available online: https://www.iith.ac.in/~{}tbr/teaching/docs/802.11-2007.pdf (accessed on 1 November 2019).
25. Outdoor Long Range Indus. Wireless Ether. Bridge AFAR Comms. Inc. Available online: http://www.afar.net/wireless/ethernet-bridge/ (accessed on 1 November 2019).
26. IEC Standards and Technical Specifications—IEC 61850-5: Comm. Requirements for Functions and Device Models. 2013. Available online: https://webstore.iec.ch/publication/6012 (accessed on 1 November 2019).
27. Aminr, M.Z.; Amirnaser, Y.; Tarlochan, S.S. A control strategy for enhanced operation of inverter-based microgrids under transient disturbances and network faults. *IEEE Trans. Power Deliv.* **2012**, *27*, 1737–1747. [CrossRef]
28. *PSCAD 4.5*; Manitoba HVDC Research Center: Winnipeg, MB, Canada, 2010; Available online: https://hvdc.ca/uploads/ck/files/reference_material/EMTDC_User_Guide_v4_3_1.pdf (accessed on 1 November 2019).